

BEARING CAPACITY OF SEWERAGE PIPELINES VS. BEDDING PARAMETERS PART I. NUMERICAL ANALYSIS

CEZARY MADRYAS, GRZEGORZ ŚMIERTKA

Institute of Civil Engineering, Division of Municipal Engineering,
Wrocław University of Technology, Wybrzeże Wyspiańskiego 27, 5-370 Wrocław, Poland.

Streszczenie: Przedstawiono wyniki modelowania zmiennych warunków posadowienia rurociągu z rur kamionkowych i wpływu tych warunków na nośność rur. Rury służą do budowy przewodów kanalizacyjnych metodami tradycyjnymi i bezwykopowymi. Celem badań symulacyjnych było wyodrębnienie najbardziej niekorzystnych schematów podparcia rur, jakie mogą wystąpić w przypadku złego wykonania podsypki, nieszczelności połączeń lub ułożenia rurociągu na podłożu o losowo zmiennych parametrach.

Abstract: Modelling results of variable bedding conditions for conventionally and trenchlessly installed stoneware pipes have been presented. The influence of the above-mentioned conditions on pipe bearing capacity has also been described. The aim of the examination was to identify the worst cases of pipe bedding resulting from wrongly prepared backfill compaction, leaking joints or pipe support of randomly variable parameters.

Резюме: Представлены результаты моделирования изменяющихся условий основания трубопровода из керамиковых труб и влияния этих условий на несущую способность труб. Трубы служат постройке канализационных проводов традиционными и бестраншейными методами. Целью имитационных исследований было выделение наиболее неблагоприятных схем крепления труб, какие могут выступить в случае плохого выполнения балласта, неплотности соединений или основания трубопровода на основании случайно изменяющихся параметров.

1. INTRODUCTION

In traditional methods of pipe bearing capacity assessment, plane stress conditions which reduce the computational model of pipe to a ring placed in soil are accepted [4]. However, in practice, longitudinal performance of pipe has frequently a significant impact on the overall pipe bearing capacity. Such situations arise for inappropriately bedded pipes under the following conditions:

- backfill is improperly compacted,
- pipe joints lost their leak-tightness during exploitation and sewage exfiltration occurs which leads to pipe washout.

In the case of pipes installed using trenchless technologies, non-uniformity of bedding conditions may be attributed to non-uniformity of surrounding ground which is uncontrolled and modified during the installation process. Therefore pipes may be locally supported by a stone, the remainder of ceiling walls or other elements termed *rigid point support*. In the case of standard trench methods, bedding conditions may

be easily made uniform by an appropriate compaction of backfill, whereas for trenchless technologies there is no such a possibility. Moreover, because of inaccessibility to the pipe capturing, it is extremely difficult to detect whether the bedding non-uniformity affects in any way the pipe bearing capacity. Actual non-uniformity of bedding conditions may be then assessed mainly on the basis of subsequent damages to the pipe resulting from exceeding the limit stress due to longitudinal performance following the installation. The problem gains in significance because of a rapid increase in trenchless technologies' popularity and their more and more frequent application to construction of underground infrastructure.

Therefore, it is vitally important to quantify a potential rise of stress due to non-uniformity of bedding conditions in order to find out whether this stress contributes significantly to the overall sewer network failure rate.

2. NUMERICAL ANALYSIS ASSUMPTIONS

In order to describe the problem, the following variables affecting the pipe bearing capacity were identified:

- pipe stiffness EI_y [kNm^2],
- pipe length L_x [m],
- external pressure q_z [kN/m],
- bedding flexibility C_L [m/kN] along the pipe axis,
- local overcompaction of bedding C_F [m/kN].

Total linear pressure q_z [kN/m] is a sum of surcharge load and ground load.

In order to obtain the maximum values of bending moments, boundary conditions representing stiff ground support were imposed on the central zone of the pipe. On the basis of parameters of joints declared by manufactures [1], [2] it was assumed that pipes were connected with hinges in the form of spigot and bell (trench methods) or couplings making a kinematic chain. A computational static model based on the aforementioned assumptions and proposed for further analysis was presented in figure 1.

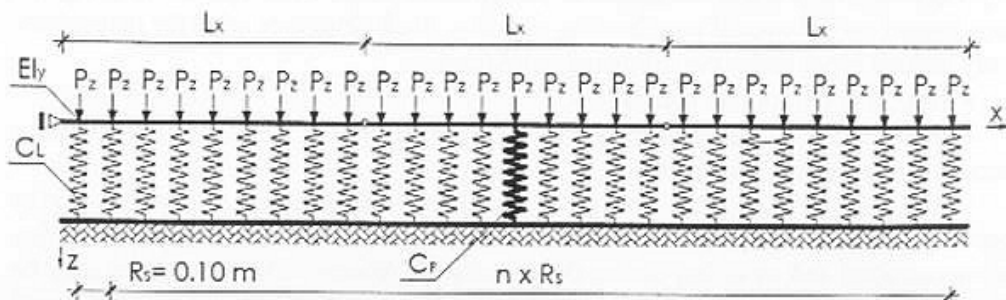


Fig. 1. Static model of pipe on flexible bedding

In the computational model adopted, the following assumptions and notation are valid:

- the elements of pipeline are supported by flexible bonds of flexibility C_L ,
- the pipeline is randomly and locally supported by bonds of flexibility C_P , and $C_P > C_L$ condition is valid herein,
- for flexibility C_L^i , the magnitude of C_P varies in the range from C_P^{i+1} to C_P^n , where $n = 19$,
- the concentrated load P_Z [kN] is a resultant force of uniformly distributed pressure q_Z [kN/m] exerted on a 0.10 m long section; the load is imposed on flexible bonds being applied,
- R_S denotes the distance between flexible bonds.

3. DATA PREPARATION FOR NUMERICAL ANALYSIS

The general formula for Winkler foundation stiffness is expressed as follows [1]:

$$K = \frac{E_0}{\omega B} \text{ [MN/m}^3\text{]}, \quad (1)$$

where:

- E_0 – deformation module for ground material [MPa],
- ω – coefficient dependent on shape and location of load [–],
- B – width (diameter) of a pipe [m].

Factor K must not be considered a material property of an individual element, but a characteristic of the foundation–bedding system, since it depends on ground properties and foundation geometry (pipe geometry in this case). In order to quantify variation of bedding stiffness, the magnitudes of K_{\max} and K_{\min} were calculated according to formula (1) and results were presented in table 1.

Table 1

Magnitudes of the coefficients K_{\max} and K_{\min}

K_{\max} [MN/m ³]	K_{\min} [MN/m ³]	$E_{0\max}$ [MPa]	$E_{0\min}$ [MPa]	ω_{\min} [–]	ω_{\max} [–]	B_{\min} [m]	B_{\max} [m]
2×10^3	–	2×10^2	–	1.00	–	0.10	–
–	10^1	–	10^1	–	2.00	–	0.50

19 magnitudes of the coefficient K assumed for computations were brought to the resultants of pipe length and pipe width B accumulated for $R_S = 0.1$ m. For the bonds obtained in this way the following parameters were assigned:

- length $L_{SP} = 1.00$ m,
- modulus of elasticity $E_{SP} = 205$ GPa,
- cross-sectional area A_{SP} [m²].

It has been assumed that bonds are linearly elastic and show infinitesimal stiffness in the X-Y directions (no buckling possibility).

Having compared the stiffness of bedding and bonds according to expression (2) the derived cross-sectional area of individual spring (3) (bond) at assumed stiffness K amounts to:

$$K \times R_s \times B = \frac{E_{SP} \times A_{SP}}{L_{SP}}, \quad (2)$$

$$A_{SP} = \frac{K \times R_s \times B \times L_{SP}}{E_{SP}} = \frac{E_0 \times R_s \times L_{SP} \times B}{E_{SP} \times \omega \times B} = \frac{E_0 \times R_s \times L_{SP}}{E_{SP} \times \omega}. \quad (3)$$

The following variables were used in calculations: the stiffness K [kN/m] or the flexibility C [m/kN] whose reciprocal dependence is expressed by the formula:

$$C = K^{-1}. \quad (4)$$

Table 2

Stiffness and flexibility of assumed bonds

K [kN/m]	C [m/kN]	E_{SP} [kN/m ²]	L_{SP} [m]	A_{SP} [m ²]	$D_{SP} = 2R_{SP}$ [m]
6.440×10^2	1.553×10^{-3}	205×10^6	1.00	3.142×10^{-6}	2.000×10^{-3}
1.449×10^3	6.901×10^{-4}	205×10^6	1.00	7.069×10^{-6}	3.000×10^{-3}
2.576×10^3	3.882×10^{-4}	205×10^6	1.00	1.257×10^{-5}	4.000×10^{-3}
4.025×10^3	2.484×10^{-4}	205×10^6	1.00	1.964×10^{-5}	5.000×10^{-3}
5.796×10^3	1.725×10^{-4}	205×10^6	1.00	2.827×10^{-5}	6.000×10^{-3}
7.889×10^3	1.268×10^{-4}	205×10^6	1.00	3.849×10^{-5}	7.000×10^{-3}
1.030×10^4	9.709×10^{-5}	205×10^6	1.00	5.027×10^{-5}	8.000×10^{-3}
1.304×10^4	7.669×10^{-5}	205×10^6	1.00	6.362×10^{-5}	9.000×10^{-3}
1.610×10^4	6.211×10^{-5}	205×10^6	1.00	7.854×10^{-5}	1.000×10^{-2}
2.516×10^4	3.975×10^{-5}	205×10^6	1.00	1.227×10^{-4}	1.250×10^{-2}
3.623×10^4	2.760×10^{-5}	205×10^6	1.00	1.767×10^{-4}	1.500×10^{-2}
4.931×10^4	2.028×10^{-5}	205×10^6	1.00	2.405×10^{-4}	1.750×10^{-2}
6.440×10^4	1.553×10^{-5}	205×10^6	1.00	3.142×10^{-4}	2.000×10^{-2}
1.006×10^5	9.940×10^{-6}	205×10^6	1.00	4.909×10^{-4}	2.500×10^{-2}
1.449×10^5	6.901×10^{-6}	205×10^6	1.00	7.069×10^{-4}	3.000×10^{-2}
1.972×10^5	5.071×10^{-6}	205×10^6	1.00	9.621×10^{-4}	3.500×10^{-2}
2.576×10^5	3.882×10^{-6}	205×10^6	1.00	1.257×10^{-3}	4.000×10^{-2}
4.025×10^5	2.485×10^{-6}	205×10^6	1.00	1.963×10^{-3}	5.000×10^{-2}
E+09	0.000	205×10^6	1.00	E+09	E+09

Mechanical parameters of the bonds obtained as above vary within the range of 0.644–25.16 [MN/m], which is presented in table 2. The values in lines 1–10 represent flexibility of ground support, whereas those in lines 2–19 show possible variations in ground support flexibility in pipe surroundings. Stiffness and flexibility of bonds located every 0.10 m were presented respectively in columns 2 and 3. In order to describe the support along the whole pipe, the values were accumulated for the unit pipe length of 1.0 m.

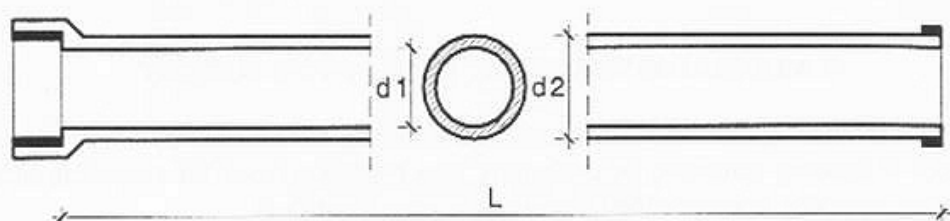


Fig. 2. Structure of a stoneware pipe

Table 3

Geometric parameters and failure forces for stoneware pipes

Diameter [mm]	Class	Strength [kN/m]	d1 [mm]	d2 [mm]	Length L [m]					
					0.50	1.00	1.25	1.50	2.00	2.50
100	–	34	100	131	–	+	+	–	–	–
125	–	34	125	158	–	+	+	–	–	–
150	–	34	150	186	–	+	+	+	–	–
200	160	32	200	242	–	+	–	+	+	–
200	240	48	200	257	–	–	–	–	+	–
250	160	40	250	299	–	–	–	–	+	–
250	240	60	250	318	–	–	–	–	+	–
300	160	48	300	355	–	–	–	–	+	–
300	240	72	300	379	–	–	–	–	+	+
350	160	56	350	417	–	–	–	–	+	–
350	160	70	350	430	–	–	–	–	+	–
400	160	64	400	486	–	–	–	–	–	+
400	200	80	400	493	–	–	–	–	–	+
450	160	72	450	548	–	–	–	–	+	–
500	120	60	500	581	–	–	–	–	–	+
500	160	80	500	609	–	–	–	–	–	+
600	95	57	600	687	–	–	–	–	–	+
150	–	–	151	186	+	+	–	–	–	–
200	–	–	200	244	–	+	–	–	–	–
250	–	–	250	322	–	+	–	–	+	–
300	–	–	300	374	–	+	–	–	+	–
400	–	–	402	516	–	+	–	–	+	–
500	–	–	503	620	–	+	–	–	+	–

Calculations were done for stoneware pipes available on the Polish market and designed for traditional and trenchless pipeline laying. Structure of pipes designed for installation in trenches is depicted in figure 2 and their main geometric parameters are presented in table 3 [3].

Lines No. 1–17 comprise data for pipes designed for traditional installation, whereas in lines 18–23 data for pipes for trenchless technologies can be found.

4. MODELLING THE WORST CASE OF PIPE SUPPORT

As was mentioned in the introduction, considering the possible modes of disturbances of bedding continuity or uniformity, two general reasons for exceeding limit stress in pipes due to longitudinal performance were identified:

- washout or compaction of soil in surroundings of pipe joints (spigot-and-bell or coupling) caused by joint leakage,
- direct or indirect (through a ground layer) pipe bedding on "rigid point of support".

Both cases led to a similar support model which was approximated by stiff support in the central zone of the pipe laying on less flexible ground compared to that near pipe ends (figure 3).

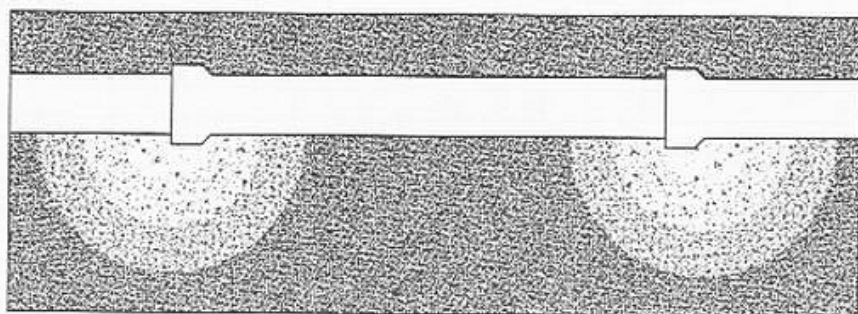


Fig. 3. Visualisation of pipe support model resulting from infiltration through leaky joints

For such a support model, the calculations for 35 pipes from the series of types shown in table 3 were done.

5. RESULTS OF ANALYSIS

The influence of a higher flexibility of local pipe support C_p at the assumed bedding flexibility C_L on the values of bending moments in the middle of pipe was presented in figure 4.

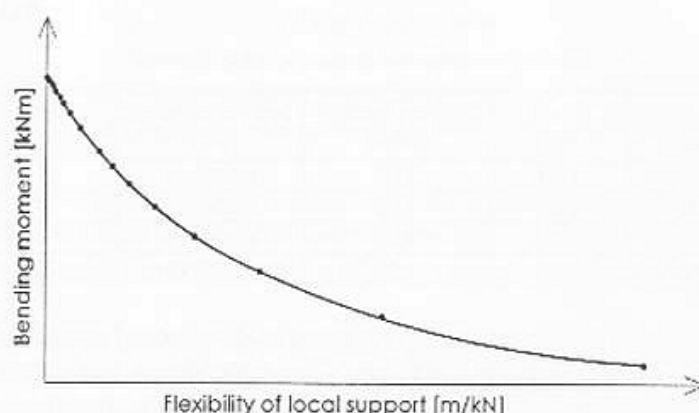


Fig. 4. Maximum bending moments vs. flexibility of local support

Mechanical response of pipe to varying bedding parameters at the assumed load was analysed based on the values of accompanying bending moments, which allowed control of correctness of modelled cases. As it is common for hyperstatic structures, an increase in element stiffness leads to an increase in bending moment. This dependence was depicted in figure 5 as an example for the pipes of the following diameters: $\varnothing 100$, $\varnothing 125$, $\varnothing 150$, $\varnothing 200$ and 1,00 m in length.

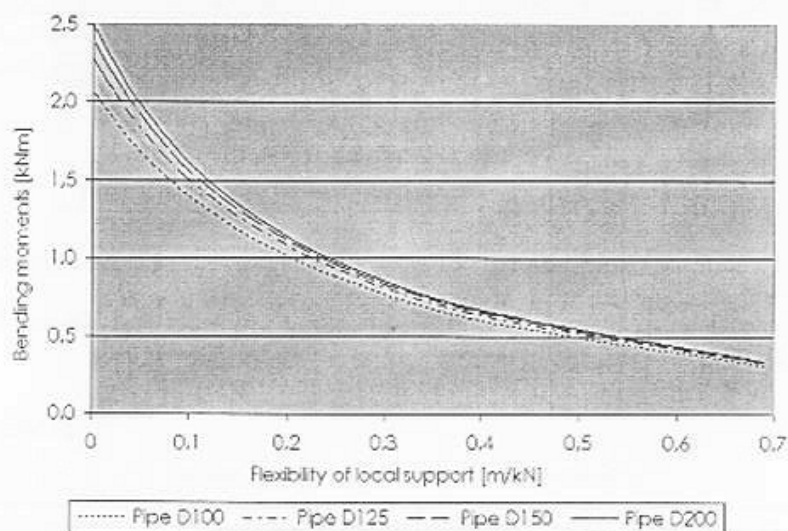


Fig. 5. Maximum bending moments vs. bedding flexibility for bedding model established

The values of maximum bending moments and stresses for the pipes shown in figure 4 are presented in table 4.

Table 4

Bending moments and stresses vs. pipe diameter

Diameter [mm]	Length [m]	Bending moment [kNm]	Section modulus [m ³]	Stress [MPa]
100	1.00	2.07	0.000146	14.18
125	1.00	2.29	0.000236	9.70
150	1.00	2.41	0.000365	6.60
200	1.00	2.51	0.000742	3.38

Different values of bending moments are expected for pipes of constant diameter and varying length, load and bedding conditions. This dependence was determined herein for pipes of $\varnothing 200$ diameter and the lengths of 1.0 m, 1.5 m and 2.0 m (figure 6).

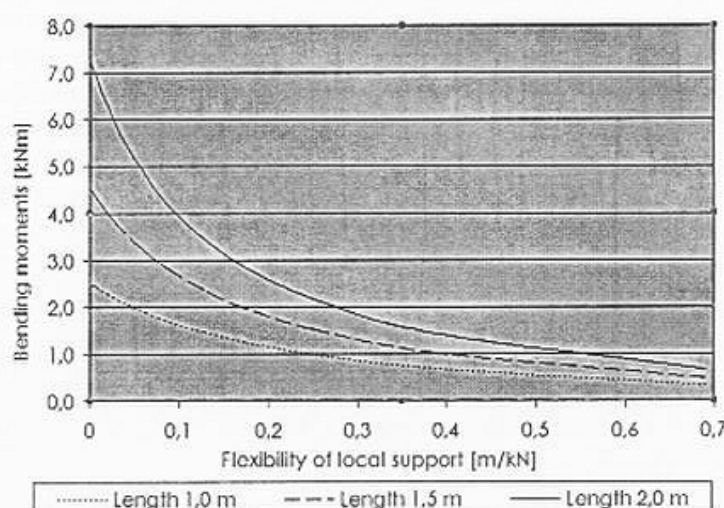


Fig. 6. Maximum bending moments vs. bedding flexibility for bedding model established

The comparison of maximum values of bending moments and stresses for pipes shown in figure 5 is presented in table 5.

Table 5

Bending moments and stresses vs. pipe length

Diameter [mm]	Length [m]	Bending moment [kNm]	Section modulus [m ³]	Stress [MPa]
200	1.00	2.51	0.000742	3.38
200	1.50	4.55	0.000742	6.13
200	2.00	7.30	0.000742	9.84

6. CONCLUSIONS

Based on the analysis carried out, the following general conclusions can be drawn:

- the pipe bearing capacity was reduced by 60% due to variations in pipe bedding parameters,
- local variations of bedding compaction rate influence the pipe bearing capacity more significantly than uniform but undercompacted or overcompacted bedding,
- higher values of internal forces and hence stresses were obtained by increasing a pipe length,
- an increase in pipe stiffness generates higher values of bending moments, but smaller values of the respective stresses due to increase in the section modulus,
- reduction of kinematic chain to only three pipe elements causes discrepancy in bending moments of the order of 6% (compared to cases No. 5, 7 and 9).

REFERENCES

- [1] BRZĄKALA W., *Fundamentowanie. Przewodnik do projektowania*, volume II, Wrocław University of Technology, Wrocław, 1990.
- [2] GABRYSZEWSKI Z., *Teoria sprężystości*, Politechnika Wrocławska, Wrocław, 1977.
- [3] Keramo Steinzeug, the guide book.
- [4] PN-EN 295-3, *Rury i kształtki kamionkowe i ich połączenia w sieci drenażowej i kanalizacyjnej. Metody badań*.
- [5] Internal report SPR 78/98 of Institute of Civil Engineering, Wrocław University of Technology, *Badania rur kamionkowych Calorfig-Keramo*.